

Effect of carbon nanotubes addition on thermoelectric properties of $Ca_3Co_4O_9$ ceramics

Ya-Nan Li(李亚男), Ping Wu(吴平), Shi-Ping Zhang(张师平), Yi-Li Pei(裴艺丽), Jin-Guang Yang(杨金光), Sen Chen(陈森), and Li Wang(王立)

Citation: Chin. Phys. B, 2022, 31 (**4**): 047203. DOI: 10.1088/1674-1056/ac4bd2
Journal homepage: http://cpb.iphy.ac.cn; http://iopscience.iop.org/cpb

What follows is a list of articles you may be interested in

Thermoelectric performance of XI_2 (X = Ge, Sn, Pb) bilayers

Nan Lu(陆楠) and Jie Guan(管杰)
Chin. Phys. B, 2022, 31 (**4**): 047201. DOI: 10.1088/1674-1056/ac474c

Thermoelectric enhancement in triple-doped strontium titanate with multi-scale microstructure

Zheng Cao(曹正), Qing-Qiao Fu(傅晴俏), Hui Gu(顾辉), Zhen Tian(田震), Xinba Yaer(新巴雅尔), Juan-Juan Xing(邢娟娟), Lei Miao(苗蕾), Xiao-Huan Wang(王晓欢), Hui-Min Liu(刘慧敏), and Jun Wang(王俊)
Chin. Phys. B, 2021, 30 (**9**): 097204. DOI: 10.1088/1674-1056/abe9a9

First principles calculations on the thermoelectric properties of bulk Au_2S with ultra-low lattice thermal conductivity

Y Y Wu(伍义远), X L Zhu(朱雪良), H Y Yang(杨恒玉), Z G Wang(王志光), Y H Li(李玉红), B T Wang(王保田)
Chin. Phys. B, 2020, 29 (**8**): 087202. DOI: 10.1088/1674-1056/ab973c

Significant role of nanoscale Bi-rich phase in optimizing thermoelectric performance of Mg_3Sb_2

Yang Wang(王杨), Xin Zhang(张忻), Yan-Qin Liu(刘燕琴), Jiu-Xing Zhang(张久兴), Ming Yue(岳明)
Chin. Phys. B, 2020, 29 (**6**): 067201. DOI: 10.1088/1674-1056/ab84cd

Thermoelectric properties of lower concentration K-doped $Ca_3Co_4O_9$ ceramics

Ya-Nan Li(李亚男), Ping Wu(吴平), Shi-Ping Zhang(张师平), Sen Chen(陈森), Dan Yan(闫丹), Jin-GuangYang(杨金光), Li Wang(王立), Xiu-Lan Huai(淮秀兰)
Chin. Phys. B, 2018, 27 (**5**): 057201. DOI: 10.1088/1674-1056/27/5/057201

Effect of carbon nanotubes addition on thermoelectric properties of $Ca_3Co_4O_9$ ceramics

Ya-Nan Li(李亚男)[1], Ping Wu(吴平)[1,†], Shi-Ping Zhang(张师平)[1], Yi-Li Pei(裴艺丽)[1], Jin-Guang Yang(杨金光)[1], Sen Chen(陈森)[1], and Li Wang(王立)[2]

[1] *Beijing Key Laboratory for MagnetoPhotoelectrical Composite and Interface Science, School of Mathematics and Physics, University of Science and Technology Beijing, Beijing* 100083, *China*

[2] *School of Energy and Environmental Engineering, University of Science and Technology Beijing, Beijing* 100083, *China*

(Received 2 October 2021; revised manuscript received 12 January 2022; accepted manuscript online 17 January 2022)

Increasing the phonon scattering center by adding nanoparticles to thermoelectric materials is an effective method of regulating the thermal conductivity. In this study, a series of $Ca_3Co_4O_9/x$ wt.% CNTs ($x = 0$, 3, 5, 7, 10) polycrystalline ceramic thermoelectric materials by adding carbon nanotubes (CNTs) were prepared with sol-gel method and cold-pressing sintering technology. The results of x-ray diffraction and field emission scanning electron microscopy show that the materials have a single-phase structure with high orientation and sheet like microstructure. The effect of adding carbon nanotubes to the thermoelectric properties of $Ca_3Co_4O_9$ was systematically measured. The test results of thermoelectric properties show that the addition of carbon nanotubes reduces the electrical conductivity and Seebeck coefficient of the material. Nevertheless, the thermal conductivity of the samples with carbon nanotubes addition is lower than that of the samples without carbon nanotubes. At 625 K, the thermal conductivity of $Ca_3Co_4O_9$/10 wt.% CNTs sample is reduced to 0.408 $W{\cdot}m^{-1}{\cdot}K^{-1}$, which is about 73% lower than that of the original sample. When the three parameters are coupled, the figure of merit of $Ca_3Co_4O_9$/3 wt.% CNTs sample reaches 0.052, which is 29% higher than that of the original sample. This shows that an appropriate amount of carbon nanotubes addition can reduce the thermal conductivity of $Ca_3Co_4O_9$ ceramic samples and improve their thermoelectric properties.

Keywords: $Ca_3Co_4O_9$, carbon nanotubes, thermal conductivity, thermoelectric properties

PACS: 72.15.Jf, 84.60.Rb, 81.05.Je, 74.25.fc **DOI:** 10.1088/1674-1056/ac4bd2

1. Introduction

With the increasingly serious energy shortage and environmental pollution, people need to find green energy and energy conversion methods. Thermoelectric materials can realize the direct conversion of thermal energy and electric energy based on Seebeck effect and Peltier effect, and they have attracted much attention in recent years.[1] The conversion efficiency of thermoelectric materials depends on the figure of merit $ZT = \sigma S^2 T/k$, where σ is the electrical conductivity, S is the Seebeck coefficient, T is the absolute temperature, and κ is the thermal conductivity.[2] It can be observed from the above formula that high-efficiency thermoelectric conversion requires high electrical conductivity and Seebeck coefficient, as well as low thermal conductivity, which is quite challenging. The optimization of one parameter of thermal conductivity or electrical conductivity usually causes the reduction of the other parameter. In recent years, compared with intermetallic thermoelectric compounds, such as Bi_2Te_3,[3] PbTe,[4] etc., thermoelectric oxide material $Ca_3Co_4O_9$ (abbreviated as CCO) has attracted extensive attention because of its good stability, convenient preparation, green environmental protection and low cost.[5] At present, the ZT value of polycrystalline $Ca_3Co_4O_9$ still cannot meet the requirements of practical application, which limits its commercial application.

$Ca_3Co_4O_9$ has monoclinic structure, and the chemical formula is $[Ca_2CoO]_{b1}[CoO_2]_{b2}$. This represents a monoclinic mismatched sandwich like structure, and a calcium salt disordered layer is mixed between CdI_2 type CoO_2 layers, extending along the c-axis. The two layers share the same lattice parameters: $a = 4.8270(5)$, $c = 10.8300(2)$, $\beta = 98.1360(1)$. The unit cell mismatch changes along the b-axis. The lattice parameter b values of Ca_2CoO_3 and CoO_2 layers are $b_1 = 4.5615(2)$ Å and $b_2 = 2.8173(1)$ Å, respectively, which are usually expressed as $[CaCoO][CoO_2]_{1.61}$.[6] The mismatch and weak connection between Ca_2CoO and CoO_2 layers enhance phonon scattering, reduce thermal conductivity, and lead to significant anisotropy.[7] Due to its unique staggered structure, in order to improve the thermoelectric performance of $Ca_3Co_4O_9$, the traditional method is to adjust the carrier concentration by doping ions at the Ca position[8–12] or Co position,[13–16] so as to affect the electric transport and phonon scattering. Another strategy is to add nano materials into $Ca_3Co_4O_9$ as the second phase. Theoretically, an appropriate number of composite nanoparticles can enhance the connectivity between grains and grain growth, improving the electrical conductivity. Due to the energy filtration effect, it may help to improve the Seebeck coefficient of the material. Simul-

†Corresponding author. E-mail: pingwu@sas.ustb.edu.cn

© 2022 Chinese Physical Society and IOP Publishing Ltd

taneously, the phonon scattering center is increased, thereby reducing the thermal conductivity. In recent years, the addition of nanoparticle materials to $Ca_3Co_4O_9$, such as SiC,[17] Bi_2O_3,[18] NaF,[19] B_4C,[20] Ag nanoparticles,[21] etc., has been used to improve the thermoelectric properties of materials. Carbon nanotube (CNT) is a low dimensional material with high conductivity and light weight. Adding carbon nanotubes to reduce the weight of materials for the application of weight sensitive thermoelectric materials is very competitive, for example, microelectronic devices, sensors, etc. Ceramic nano powders are widely used as nano dispersions of thermoelectric nanocomposites because of their low thermal conductivity, but the nanocomposites prepared from these nano dispersions show serious conductivity degradation. In contrast, carbon nanotubes are excellent nano dispersions of thermoelectric nanocomposites because CNTs have high conductivity, and their dispersion in the thermoelectric matrix will not deteriorate the conductivity to the extent caused by ceramic nano powder. Yeo *et al.*[22] added 0.12% CNTs to $(Bi_{0.2}Sb_{0.8})_2Te_3$, the thermal conductivity of the composite was significantly lower than that of the matrix, which increased the ZT value by 34%. Kim *et al.*[23] found that the thermal conductivity decreased significantly by compounding $Bi_{0.5}Sb_{1.5}Te_3$ with porous carbon nanomaterials. Theoretically, although carbon nanotubes have high thermal conductivity, the interface between carbon nanotubes and matrix can increase the phonon scattering at the interface and reduce the thermal conductivity, which is expected to improve the ZT value of the material. Tang *et al.* previously studied the effect of carbon nanotubes addition on the thermoelectric properties of $Ca_3Co_4O_9$ at low temperature.[24] The thermoelectric properties of carbon nanotubes doped at room temperature and higher temperature have not been studied.

In this work, $Ca_3Co_4O_9/x$ wt.% CNTs ($x = 0$, 3, 5, 7, 10) composite thermoelectric materials were prepared by sol-gel method. The effects of adding carbon nanotubes on the electrical properties and thermal conductivity of $Ca_3Co_4O_9$ were systematically investigated.

2. Experimental details

$Ca_3Co_4O_9$ powder samples were prepared by sol-gel method. Weigh the precursor raw materials Ca $(NO_3)_2{\cdot}4H_2O$ and CO $(NO_3)_2{\cdot}6H_2O$ at a certain stoichiometric ratio, dissolve the raw materials in deionized water and mix evenly, add a certain amount of citric acid, heat and stir continuously at 352 K until sol is formed. The sol was dried at 393 K for 12 h to obtain the precursor. The precursor was fully ground and sintered at constant temperature of 1073 K for 12 h after self-propagating treatment. After sintering, the powder sample was evenly mixed with carbon nanotubes (CNTs; 0 wt.%, 3 wt.%, 5 wt.%, 7 wt.%, 10 wt.%) with a certain mass ratio, and then pressed under the pressure of 30 MPa. Crystallographic structure analysis was performed by Rigaku D/max2500 X diffractometer with Cu $K\alpha$ ray ($\lambda = 1.54056$ Å) (40 kV, 200 mA), step size 0.01°, conventional 2θ of 10°–60°. The phase composition of the sample was analyzed by angle range diffraction spectrum. The microstructure of the samples was observed by field emission scanning electron microscopy (FE-SEM, Zeiss supra55). The Seebeck coefficient/electrical conductivity measurement system (Netzsch SBA458) was used to measure the electrical conductivity and Seebeck coefficient of the sample in argon atmosphere. The thermal conductivity of the sample was obtained according to $k = DC_pd$, where d is the geometric density of the sample. The diffusion coefficient D (Netzsch instruments/LAF457) perpendicular to the pressure direction of the sample was obtained by laser scattering method.

3. Results and discussion

3.1. Phase composition and microstructure

The phase purity and crystallinity of $Ca_3Co_4O_9$ samples with carbon nanotubes addition of different mass ratios were characterized by XRD. Figure 1 shows the XRD spectra of all samples. All samples are single-phase, and the major crystal phase matches with the standard JCPDS card (No. 21-0139) of $Ca_3Co_4O_9$. No other peaks are detected, indicating that the purity of all samples is very high, and the content of carbon nanotubes is relatively small. It can also be seen from the figure that the diffraction peak in the (00l) plane is relatively strong, while other peaks are relatively weak. The results show that the samples have obvious preferred orientation in the c direction, which is mainly caused by the preferential growth of grains on the plane perpendicular to the pressure direction during sintering. Simultaneously, with the increase of the amount of carbon nanotubes, the orientation of the sample in the (00l) direction decreases.

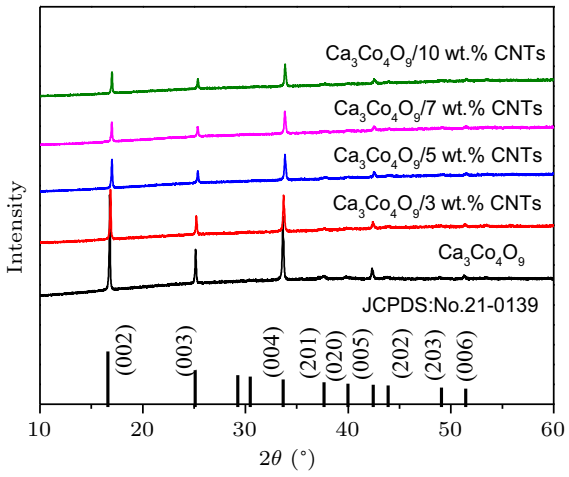


Fig. 1. XRD pattern of $Ca_3Co_4O_9/x$ wt.% CNTs ($x = 0$, 3, 5, 7, 10) sample.

Figures 2(a)–2(e) show the morphology of the samples added with different proportions of carbon nanotubes. It can be observed from the figure that the sample presents a sheet shape. It is found that the grain size does not change significantly with the increase of carbon nanotubes. The average particle size of the sample is 700–800 nm. Figure 2(f) shows the morphology of the sample with carbon nanotubes doping of 10 wt.% at a higher multiple. The filamentous carbon nanotubes in the sample are circled with a blue circle. The density and atomic ratio of $Ca_3Co_4O_9/x$ wt.% CNTs ($x = 0$, 3, 5, 7, 10) samples are provided in Table 1. The density of the sample decreases with the increase in the content of carbon nanotubes (the theoretical density of $Ca_3Co_4O_9$ is 4.68 g/cm^3).[25] After normalizing the atomic ratio, the content of carbon atoms in the sample increases with the increase of the amount of carbon nanotubes.

Table 1. Density and atomic ratio of $Ca_3Co_4O_9/x$ wt.% CNTs ($x = 0$, 3, 5, 7, 10) series samples.

Sample	Density (g/cm^3)	Atomic ratio		
		Ca	Co	C
0 wt.%	3.964	3.00	3.75	0
3 wt.%	3.409	3.00	4.00	1.55
5 wt.%	3.067	3.00	3.83	2.20
7 wt.%	2.874	3.00	3.95	2.21
10 wt.%	2.608	3.00	3.84	2.28

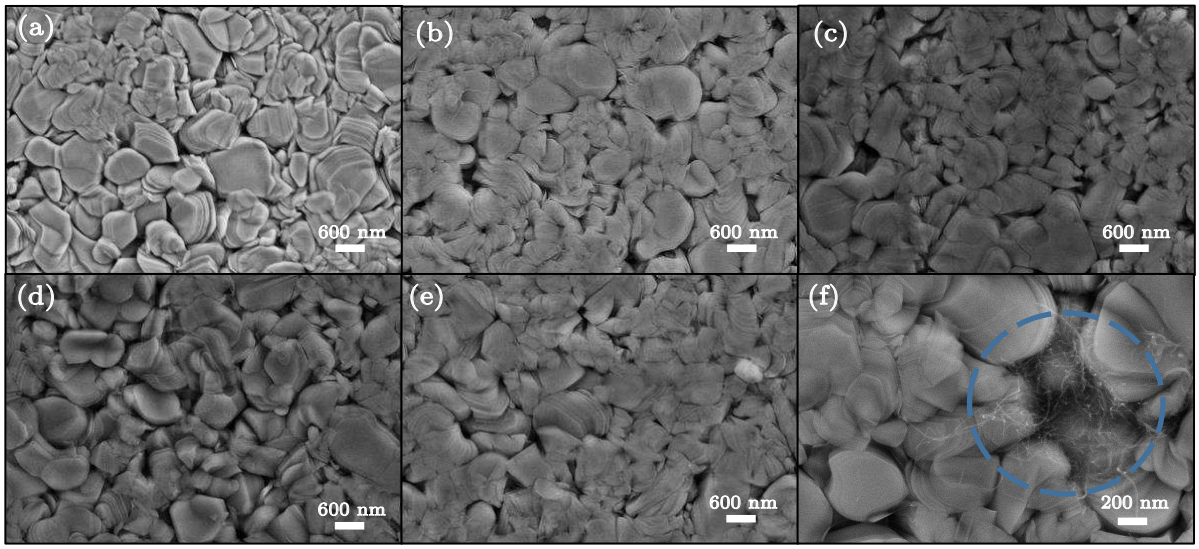


Fig. 2. SEM images of sintered sample surfaces: (a) $Ca_3Co_4O_9$, (b) $Ca_3Co_4O_9$/3 wt.% CNTs (c) $Ca_3Co_4O_9$/5 wt.% CNTs, (d) $Ca_3Co_4O_9$/7 wt.% CNTs, (e) $Ca_3Co_4O_9$/10 wt.% CNTs and (f) filamentous carbon nanotubes in $Ca_3Co_4O_9$/10 wt.% CNTs are circled with a blue circle.

3.2. Electrical transport properties

The relationship between electrical conductivity and temperature of $Ca_3Co_4O_9/x$ wt.% CNTs ($x = 0$, 3, 5, 7, 10) samples are exhibited in Fig. 3. Due to the limitation of the stability of carbon nanotubes, the test mainly studies the thermoelectric properties of samples from room temperature to 625 K. It can be observed from the figure that the electrical conductivity of all samples increases with the increase of temperature in the temperature range of 275 K to 625 K, showing significant semiconductor behavior. However, the conductivity of the sample with carbon nanotubes addition is significantly lower than that of the original sample. Although carbon nanotubes have high conductivity, it is mainly reflected along its length. In this study, the orientation of carbon nanotubes added to $Ca_3Co_4O_9$ is random, then its excellent conductivity cannot be brought into full play. The relationship between conductivity and resistivity can be expressed as $\sigma = 1/\rho$. Adding carbon nanotubes to $Ca_3Co_4O_9$ sample introduces pore structure and interface, which increases the electron scattering center of the composite sample, increases the resistivity of the sample, that is, the electrical conductivity decreases, and the electrical conductivity of the composite decreases with the increase of carbon nanotube content.

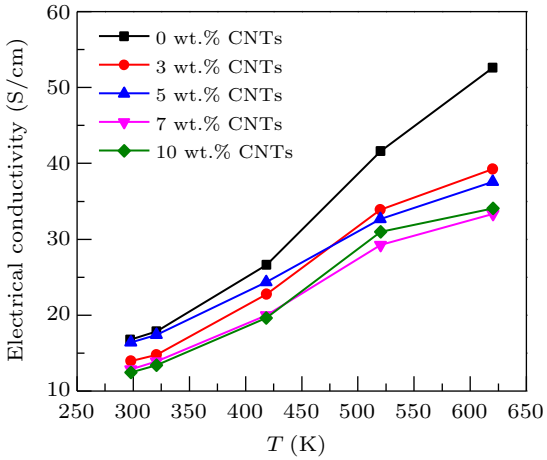


Fig. 3. Relationship between the electrical conductivity and temperature of $Ca_3Co_4O_9/x$ wt.% CNTs ($x = 0$, 3, 5, 7, 10) series samples.

Figure 4 shows the relationship between Seebeck coefficients and temperature of $Ca_3Co_4O_9$ samples with different contents of carbon nanotubes. The Seebeck coefficients of all samples in the figure increase with the increase of temperature. The Seebeck coefficients of all samples are positive, indicating

that the samples are p-type semiconductors, dominated by hole conduction. The Seebeck coefficient increases monotonically with the increase of temperature, which may be related to the phonon traction effect, that is, the phonons in the semiconductor flow from the high-temperature end to the low-temperature end. Through the collision with the carriers, the phonons transfer energy to the carriers, forming the flow of carriers in the same direction as the phonon flow, to improve the Seebeck coefficient. Simultaneously, it can be observed from the figure that the Seebeck coefficient of the sample decreases with the increase of carbon nanotubes content. At 625 K, the Seebeck coefficient of the $Ca_3Co_4O_9$/10 wt.% CNTs sample decreases to 136.85 μV/K, compared with 82.02 μV/K of the undoped samples, reduced by about 40%. For the composite semiconductor material of two substances, the Seebeck coefficient can be expressed as[26]

$$S_{\mathrm{TOT}} = \sum_i \sigma_i S_i / \sum_i \sigma_i, \tag{1}$$

where S_{TOT} represents the total Seebeck of the sample, σ_i represents the conductivity of different substances, and S_i represents the Seebeck coefficient of different substances. It can be seen from the formula that the conductivity has a great influence on the Seebeck coefficient. Carbon nanotubes have higher conductivity, that is, the denominator becomes larger, while the Seebeck coefficient of carbon nanotubes is smaller, and the molecular change is small.[27] Thus, the Seebeck coefficient of the composite sample is reduced.

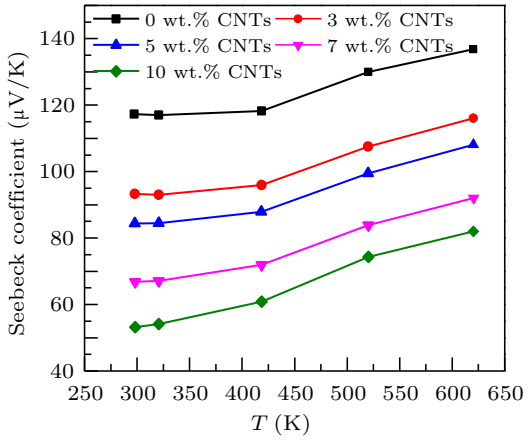


Fig. 4. Relationship between the Seebeck coefficient and temperature of $Ca_3Co_4O_9/x$ wt.% CNTs ($x = 0$, 3, 5, 7, 10) series samples.

Based on the measurement results of electrical conductivity and Seebeck coefficient, to evaluate the electrical properties of thermoelectric materials, the electrical properties part of $ZT = \sigma S^2 T/k$ is used, σS^2, which is called the power factor PF ($PF = \sigma S^2$) of the material. The calculated power factor of $Ca_3Co_4O_9/x$ wt.% CNTs series samples is provided in Fig. 5. The power factor increases with the increase of temperature which can be attributed the joint influence of electrical conductivity and Seebeck coefficient. In the whole temperature range, the power factor of the samples with carbon nanotubes added is lower than that of the original samples. At 625 K, the power factor of the undoped samples is 0.98 μW/cm·K^2. The power factor of $Ca_3Co_4O_9$/10 wt.% CNTs samples decreases to 0.22 μW/cm·K^2. The above results show that doping carbon nanotubes will reduce the electrical properties of the materials.

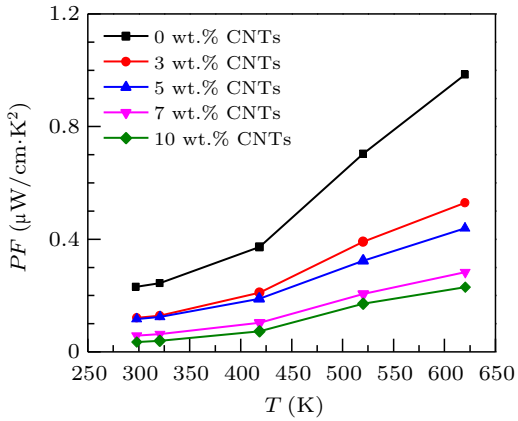


Fig. 5. Relationship between the power factor and temperature of $Ca_3Co_4O_9/x$ wt.% CNTs ($x = 0$, 3, 5, 7, 10) series samples.

3.3. Thermal transport properties

Figure 6(a) shows the variation of the total thermal conductivity of the sample with temperature. The thermal conductivity of the sample with carbon nanotubes addition is significantly lower than that of the original sample. And the thermal conductivity decreases with the increase of the content of carbon nanotubes. For $Ca_3Co_4O_9/x$ wt.% CNTs system, in general, the total thermal conductivity k of the sample consists of two parts: the carrier thermal conductivity k_c and phonon thermal conductivity k_p, i.e., $k = k_c + k_p$. The carrier thermal conductivity k_c is related to the electrical conductivity via the Wiedemann–Franz equation, $k_c = LT\sigma$, where L is the Lorenz constant ($L = 2.45 \times 10^{-8}$ V^{-2}·K^{-2}), and the calculated value of k_c can be ignored for its relatively small value (Fig. 6(b)). Therefore, k mainly depends on k_p (Fig. 6(c)). In the low order approximation, $k_p = 1/3cvl_p$, where c, v and l_p represent the specific heat capacity, phonon propagation velocity and average free path, respectively. Generally, doping will increase c and decrease v and l_p. Moreover, the phonon propagation velocity is positively correlated with the average free path of the phonon. At 625 K, the thermal conductivity of the sample decreases from 1.527 W·m^{-1}·K^{-1} of $Ca_3Co_4O_9$ to 0.408 W·m^{-1}·K^{-1} of $Ca_3Co_4O_9$/10 wt.% CNTs, which is decreased by about 73%.

The main factors affecting the thermal conductivity of composites include their own thermal conductivity, particle distribution of added phase, interfacial thermal resistance,

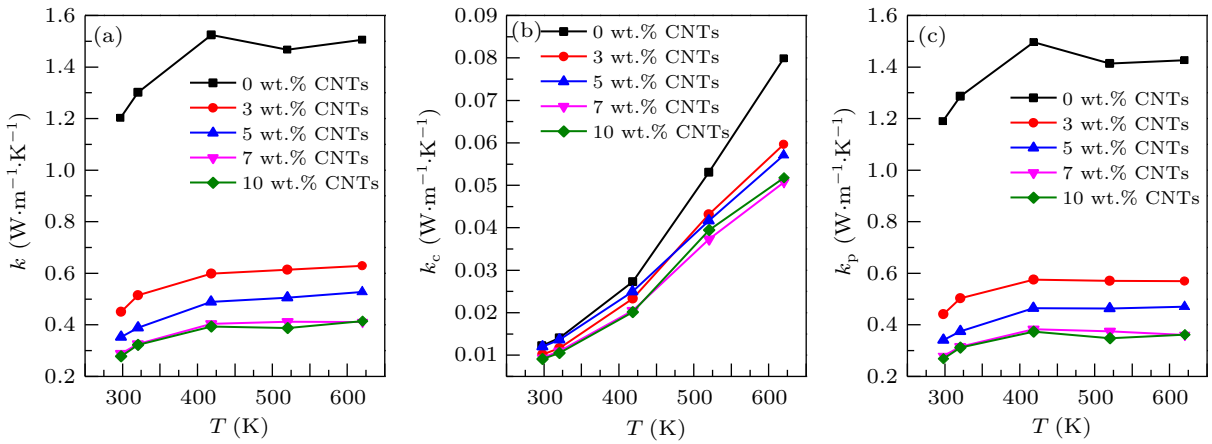


Fig. 6. Relationship between (a) total thermal conductivity k, (b) carrier thermal conductivity k_c and (c) phonon thermal conductivity k_p of $Ca_3Co_4O_9/x$ wt.% CNTs ($x = 0, 3, 5, 7, 10$) series samples with temperature.

porosity and so on. The thermal conductivity of carbon nanotubes is relatively high. The thermal conductivity of multi walled carbon nanotubes reaches 600–4000 W·m^{-1}·K^{-1} at room temperature. When adding high thermal conductivity carbon nanotubes to $Ca_3Co_4O_9$, it is generally believed that the thermal conductivity will increase, while the actual measurement results decrease with the addition of carbon nanotubes. In this study, the particle phase of the composites obtained by fully mixing carbon nanotubes and $Ca_3Co_4O_9$ can be regarded as uniformly distributed, so the effect of particle distribution on it can be ignored.

According to Matthiessen's law, the phonon thermal conductivity mainly depends on point defect scattering, grain boundary scattering, phonon–phonon scattering and resonance scattering.[28,29] The existence of composite interface will inevitably affect the thermal conductivity. Pang *et al.* optimized the series parallel model based on the effective medium thermal conductivity theory, and gave the effective thermal conductivity of composite elements with interfacial thermal resistance k_{com} as[30]

$$k_{com} = k_2 + \frac{\pi B^{-1}}{A} - \pi k_2 B^{-2} + \frac{\pi\left(\frac{B}{k_2} + \frac{2R_B}{R}\right)\ln\left(\frac{\frac{B}{k_2}+\frac{2R_B}{R}}{2A+\frac{B}{k_2}+\frac{2R_B}{R}}\right)}{2BA^2}, \tag{2}$$

with

$$A = \frac{1}{k_1} - \frac{1}{k_2}, \quad B = \sqrt[3]{\frac{4\pi}{3V_1}},$$

where k_2 is the thermal conductivity of the matrix material, k_1 is the thermal conductivity of the additive, V_1 is the volume fraction of the added phase, R is the diameter of the added phase particles, and R_B is the interfacial thermal resistance of the added phase in the composite. In this study, the particle size of $Ca_3Co_4O_9$ is about 700 nm, while the diameter of carbon nanotubes is only about 5 nm, which is much smaller than that of $Ca_3Co_4O_9$ and can be regarded as spherical particles. The effect of carbon nanotube addition on the effective thermal conductivity of $Ca_3Co_4O_9$ material can be discussed by using the model of formula (2). Therefore, for carbon nanotubes and $Ca_3Co_4O_9$ matrix composites, k_2 is the thermal conductivity of the matrix $Ca_3Co_4O_9$ without carbon nanotubes, k_1 is the thermal conductivity of carbon nanotubes, the carbon nanotubes added in the experiment are double-walled carbon nanotubes, the thermal conductivity is about 3000 W·m^{-1}·K^{-1}, V_1 is the volume fraction of carbon nanotubes, R is the diameter of carbon nanotubes (5 nm), and R_B is the interfacial thermal resistance of carbon nanotubes in the composites, According to a report of Cahill and Keblinski research group, the interfacial thermal resistance of carbon nanotubes is about 8.33×10^{-8} m^2·K·W^{-1}.[31] By substituting the corresponding value into formula (2), the effective thermal conductivity k_{com} of $Ca_3Co_4O_9$ composites with different amounts of carbon nanotubes can be calculated when considering the interfacial thermal resistance. The calculation results are shown in Fig. 7.

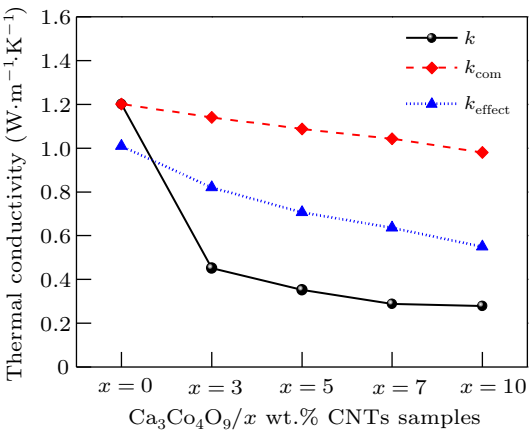


Fig. 7. Relationship among k_{com}, k_{effect} and k of $Ca_3Co_4O_9/x$ wt.% CNTs ($x = 0, 3, 5, 7, 10$) series samples.

For ceramic samples, the effect of pores on the thermal conductivity of materials cannot be ignored. To study the effect of pores on thermal conductivity, Pang *et al.* transformed the ideal composite into a single-phase solid material with effective thermal conductivity of k_{com} and regarded the pore phase as one phase to build a model based on the model of

formula (2), and deduced that the effective thermal conductivity (k_{effect}) of the composite with voids and interfacial thermal resistance is[30]

$$\frac{1}{k_{\text{effect}}} = \frac{1-1.24\xi^{\frac{1}{3}}}{k_{\text{com}}} + \frac{1}{0.65(k_{\text{air}}-k_{\text{com}})\xi^{\frac{1}{3}} + 0.81k_{\text{com}}\xi^{-\frac{1}{3}}}, \tag{3}$$

where k_{air} is the thermal conductivity of the stomatal phase, ξ is the proportion of pore phase in the unit, that is, porosity $\xi = (\rho_0 - \rho_i)/\rho_0$, ρ_0 is the theoretical density of the base material, ρ_i is the density of each sample. In this study, the carbon nanotube with interface and $Ca_3Co_4O_9$ composite discussed in formula (2) are regarded as a single phase, and the pores are regarded as the second phase, that is, k_{air} is the thermal conductivity of the pore phase (0.023 $W{\cdot}m^{-1}{\cdot}K^{-1}$), ρ_0 is the theoretical density of $Ca_3Co_4O_9$ (4.68 g/cm^3), ρ_i is given in Table 1. Bring the above values into formula (3) to calculate the effective thermal conductivity of the composite containing pores and interfaces. The calculation results are given in Fig. 7.

As shown in Fig. 7, when only the interfacial thermal resistance is considered, the effective thermal conductivity k_{com} value of carbon nanotubes and $Ca_3Co_4O_9$ composites decreases with the increase of the amount of carbon nanotubes, which is consistent with the experimental k. The results show that the addition of carbon nanotubes into the interface hinders heat transfer and reduces the thermal conductivity of the composites. When the effects of interfacial thermal resistance and pores on the effective thermal conductivity k_{effect} of the composites are considered at the same time, the effect value also decreases with the increase of the amount of carbon nanotubes, and the decreasing trend is greater than k_{com} and closer to the experimental value k, indicating that pores have a great influence on the effective thermal conductivity of the composites. In conclusion, adding carbon nanotubes to $Ca_3Co_4O_9$ introduces interfacial thermal resistance and pores, which plays an important role in reducing the thermal conductivity, indicating that adding carbon nanotubes is one of the effective ways to reduce the thermal conductivity of $Ca_3Co_4O_9$.

3.4. Dimensionless figure of merit

Figure 8 shows the relationship between the ZT value and temperature of $Ca_3Co_4O_9/x$ wt.% CNTs (x = 0, 3, 5, 7, 10) samples . The ZT value is the result of the coupling of electrical conductivity, Seebeck coefficient and thermal conductivity. It can be seen from the calculation results that the ZT values of the $Ca_3Co_4O_9$/3 wt.% CNTs and $Ca_3Co_4O_9$/5 wt.% CNTs samples increase significantly, and that of $Ca_3Co_4O_9$/7 wt.% CNTs has little change. With the increase of the content of carbon nanotubes, the ZT value of the $Ca_3Co_4O_9$/10wt.% CNTs sample decreases. At 625 K, the ZT value of the sample with the addition content of 3% is the highest, reaching 0.052. Compared with pure $Ca_3Co_4O_9$ samples at the same temperature, the ZT value is increased by 29%. The sample with 3 wt.% CNTs has the best thermoelectric performance at 625 K. The above results show that an appropriate amount of carbon nanotubes is an effective method to improve the thermoelectric properties of $Ca_3Co_4O_9$.

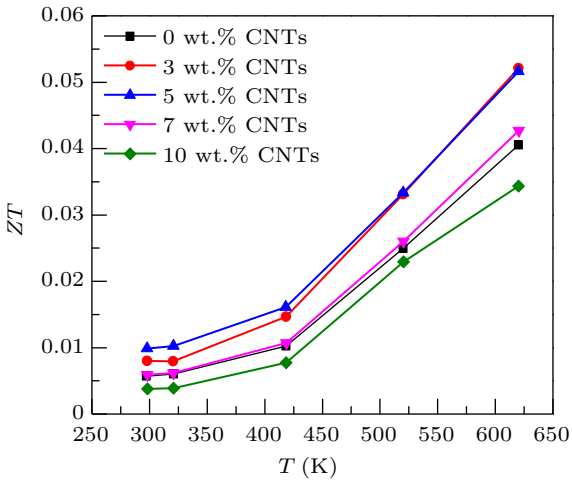


Fig. 8. Relationship between the ZT value and temperature of $Ca_3Co_4O_9/x$ wt.% CNTs (x = 0, 3, 5, 7, 10) series samples .

4. Conclusions

We systematically studied the thermoelectric properties of $Ca_3Co_4O_9/x$ wt.% CNTs (x = 0, 3, 5, 7, 10) composite samples prepared by sol-gel method. XRD and SEM showed that the samples were single phase and showed sheet like morphology. The electrical conductivity and Seebeck coefficient of all samples with carbon nanotubes addition were lower than those of the original sample. Proper addition of carbon nanotubes can effectively reduce its thermal conductivity. At 625 K, the thermal conductivity of the sample ($Ca_3Co_4O_9$/10 wt.% CNTs) decreased from 1.527 $W{\cdot}m^{-1}{\cdot}K^{-1}$ of undoped samples to 0.408 $W{\cdot}m^{-1}{\cdot}K^{-1}$, which decreased by about 73%. When the addition content was 3%, the ZT value reached 0.052, which was 29% higher than that the original sample. These show that an appropriate amount addition of CNTs can reduce the thermal conductivity of $Ca_3Co_4O_9$ ceramic samples and improve the thermoelectric properties.

Acknowledgement

This work was supported by the National Natural Science Foundation of China (Grant No. 51836009).

References

[1] Sootsman J R, Chung D Y and Kanatzidis M G 2009 *Angew. Chem. Int. Edit.* **48** 8616

[2] Rowe D M 2006 *Thermoelectrics Handbook: Macro to Nano* (Taylor & Francis: CRC Press)

[3] Romanenko A I, Chebanova G E, Drozhzhin M V, Katamanin I N, Komarov V Y, Han M K, Kim S J, Chen T and Wang H C 2021 *J. Am. Ceram. Soc.* **104** 6242

[4] Adam A M, Ibrahim E, Panbude A, Jayabal K and Diab A K 2021 *J. Alloys Compd.* **872** 159630

[5] Ge Z H, Zhao L D, Di W, Liu X and He J 2016 *Mater. Today* **19** 227

[6] Masset A C, Michel C, Maignan A, Hervieu M, Toulemonde O, Studer F, Raveau B and Hejtmanek J 2000 *Phys. Rev. B* **62** 166

[7] Yin Y, Tudu B and Tiwari A 2017 *Vacuum* **146** 356

[8] Madre M A, Urrutibeascoa I, Garcia G, Torres M A, Sotelo A and Diez J C 2019 *J. Electron Mater.* **48** 1965

[9] Madre M A, Rasekh S, Torres M A, Diez J C and Sotelo A 2018 *Adv. Appl. Ceram.* **117** 142

[10] Li Y N, Wu P, Zhang S P, Chen S, Yan D, Yang J G, Wang L and Huai X L 2018 *Chin. Phys. B* **27** 057201

[11] Hira U, Han L, Norrman K, Christensen D V, Pryds N and Sher F 2018 *Rsc. Adv.* **8** 12211

[12] Cha J S, Choi S M, Kim G H, Kim S J and Park K 2018 *Ceram. Int.* **44** 6376

[13] Li Y N, Wu P, Zhang S P, Yang J G, Yan D and Huai X L 2020 *J. Mater. Sci. Mater. Electron.* **31** 5353

[14] Butt S, Liu Y C, Lan J L, Shehzad K, Zhan B, Lin Y and Nan C W 2014 *J. Alloys Compd.* **588** 277

[15] Sun Y and Song W 2006 *J. Appl. Phys.* **99** 073906

[16] Madre M A, Rasekh Sh, Torres M A, Diez J C and Sotelo A 2018 *Adv. Appl. Ceram.* **117** 142

[17] Wang X, Liu X C, Yan W, Hou S and Liu X 2019 *J. Alloys Compd.* **785** 698

[18] Shi Z M, Gao F, Zhu J H, Xu J, Zhang Y, Gao T and Qin M J 2019 *J. Materiomics* **5** 711

[19] Porokhin S, Shvanskaya L, Khovaylo V and Vasiliev A 2017 *J. Alloys Compd.* **695** 2844

[20] Amaveda H, Mora M, Dura O J, Torres M A, Madre M A, Marinel S and Sotelo A 2021 *J. Eur. Ceram. Soc.* **41** 402

[21] Kahraman F, Madre M A, Rasekh S, Salvador C, Bosque P, Torres M A, Diez J C and Sotelo A 2015 *J. Eur. Ceram. Soc.* **35** 3835

[22] Yeo Y H and Oh T S 2014 *Mater. Res. Bul.* **58** 54

[23] Kim S T, Park J M, Park K I, Chun S F, Lee H S, Choi P P and Yi S 2021 *J. Mater. Sci. Technol.* **94** 175

[24] Tang G D, Yang W C, Wen J F, Wu Z C, Fan C and Wang Z H 2015 *Ceram. Int.* **41** 961

[25] Schulz T and Töpfer J 2016 *J. Alloys Compd.* **659** 122

[26] Barnard R D and Cannella V 1974 *Phys. Today* **27** 52

[27] Miao T, Ma W, Xing Z, Wei J and Sun J 2013 *Appl. Phys. Lett.* **102** 053105

[28] Lundstrom M 2000 *Fundamentals of Carrier Transport*, 2nd edn (Cambridge: Cambridge University Press) pp. 54–118

[29] Chen G 2005 *Nanoscale energy transport and conversion: a parallel treatment of electrons, molecules, phonons, and photons* (Oxford: Oxford University Press)

[30] Pang X M, Zhou J Q, Yang J X and Liao M H 2016 *The Chinese Journal of Nonferrous Metals* **26** 1668

[31] Huxtable S T, Cahill D G, Shenogin S, Xue L, Ozisik R, Barone P, Usrey M, Strano M S, Siddons G and Shim M 2003 *Nat. Mater.* **2** 731